What is a Diode Laser Oscillator?

Larry A. Coldren, *Life Fellow, IEEE*

***Abstract*—This article attempts to summarize some of the discussion that took place during the "Rump" Session at the 2012 International Semiconductor Laser Conference. The discussion mostly centered around the topic of how one can identify lasing in a given structure, and how one might differentiate between the different kinds of possible light emission.**

***Index Terms*—diode lasers, lasing, coherence**

I. INTRODUCTION

As the first speaker, I attempted to lay some familiar elementary groundwork for what one commonly encounters as the definition of lasing and the identification of the lasing threshold in diode lasers. To no ones surprise, I used a few equations and plots from our textbook on Diode Lasers and Photonic Integrated Circuits [1]. I also indicated my bias toward devices that had at least some future hope of having the desirable properties that we look for in diode lasers. That is, high-efficiency, high reliability, low cost, direct current pumping, a directed output beam, high direct-modulation speed, reasonable output power, and relatively good coherence in addition to small size. Integrability with other optics and perhaps electronic ICs has also become a key attribute as we consider future uses of small, efficient devices.

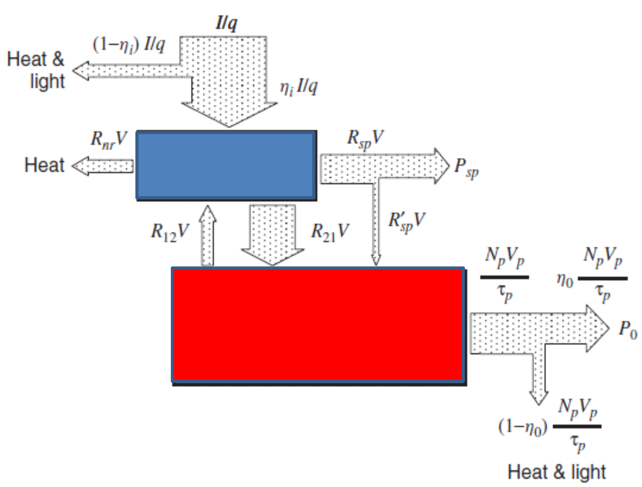

Fig. 1. Diode laser model illustrating the flow of input current, I, to create carriers in a carrier reservoir and the interaction of this reservoir with a single photon reservoir that provides an output power, P_0. The carrier reservoir (active region) of volume V physically overlaps the photon reservoir of volume V_p to enable the spontaneous and stimulated generation of photons shown by the interconnecting flow arrows. For multimode lasers there are multiple photon reservoirs coupled to the single carrier reservoir.

L. A. Coldren is with the Departments of Electrical & Computer Engineering and Materials at the University of California, Santa Barbara, CA 93106 (e-mail: coldren@ece.ucsb.edu).

II. DYNAMIC CARRIER/PHOTON FLOW

Figure 1 is Fig. 5.1 in ref. 1. From the rates of flow, R_j, of charge carriers and photons across the various boundaries, this diagram not only allows for the derivation of rate equations from which the static and dynamic properties of diode lasers can be determined, but by including 'shot noise' at all interfaces, it also provides the basis for the derivation of the Relative Intensity Noise (RIN) and linewidth of these devices [1]. It specifically illustrates the creation of charge carriers in a Carrier Reservoir (assumed equal holes and electrons) from a current pumping source. [For optical pumping the picture doesn't change; one just replaces I by the optical pump power, P_p, q to $h\nu$, and interprets η_i differently at the top of the diagram.] The carriers are lost both radiatively, R_{sp}, and nonradiatively, R_{nr}, and they interact with the Photon Reservoir via stimulated recombination, R_{21}, and generation, R_{12}. A small portion of the radiative recombination, $R'_{sp} = \beta R_{sp}$ is coupled into the single optical mode, which is implicitly assumed by the single photon reservoir. The number of photons in the mode, N_pV_p, decay with a time constant τ_p; a fraction, η_0, are coupled into a desired output pathway to provide the output power $P_0 = \eta_0 h\nu N_p V_p / \tau_p$.

III. OUTPUT CHARACTERISTICS

By inspection we can write down a set of rate equations for the carrier (electrons = holes) and photon densities from Fig. 1. Then, to obtain an asymptote above the lasing threshold, we note that the steady-state modal gain cannot exceed the modal loss. In fact, it really never quite equals it because of the generally small amount of spontaneous emission, $R'_{sp} = \beta R_{sp}$, coupled into the mode as well. But, to get the asymptote, we neglect this spontaneous emission in the photon rate equation and solve for the power into the single lasing mode, P_0. We can also solve for the total spontaneous emission P_{sp} above the lasing threshold from the carrier rate equation. Then, for ($I > I_{th}$) we have,

$$P_0 = \eta_i \eta_0 \frac{h\nu}{q}(I - I_{th}) \quad \text{and} \quad P_{sp} = \eta_i \eta_r \frac{h\nu}{q} I_{th} \qquad (1)$$

where η_r is the fraction of carrier recombination that is radiative. Note, that because the gain clamps, the carrier density and P_{sp} should also clamp at threshold. However, if there is a large leakage current or poor injection efficiency, there can be additional spontaneous emission from this current outside of our single reservoir model.

Now, we can also calculate the below-threshold asymptote for the *single lasing mode*, by assuming only spontaneous

This article has been accepted for publication in a future issue of this journal, but has not been fully edited. Content may change prior to final publication.

emission into only this mode from the photon rate equation and neglecting stimulated emission:

$$P_0(I < I_{th}) = \eta_i \eta_0 \eta_r \beta h\nu / q \qquad (2)$$

An approximate $P - I$ characteristic for diode lasers with a relatively small β, say $< 10^{-3}$, can be obtained by just plotting the asymptotes, Eqns. (1) and (2), on a linear scale. This is generally true for most diode lasers unless quite small. For example, this holds for good VCSELs with diameters > 6 µm. However, for larger β, the juncture between the two equations becomes noticeably less abrupt.

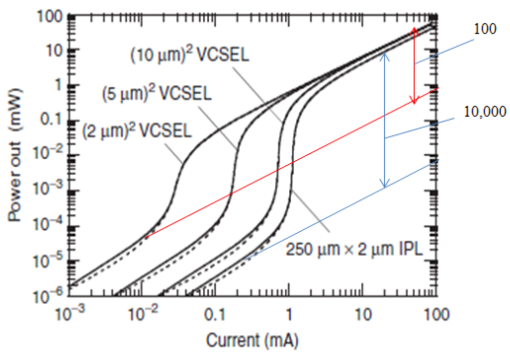

Fig. 2. Log-log output power vs current calculations for various lasers. Only one optical mode is included. Numbers in the right margin are ratios of slopes. Dashed curves assume a constant β, the solid curves use exact mode coupling approach.

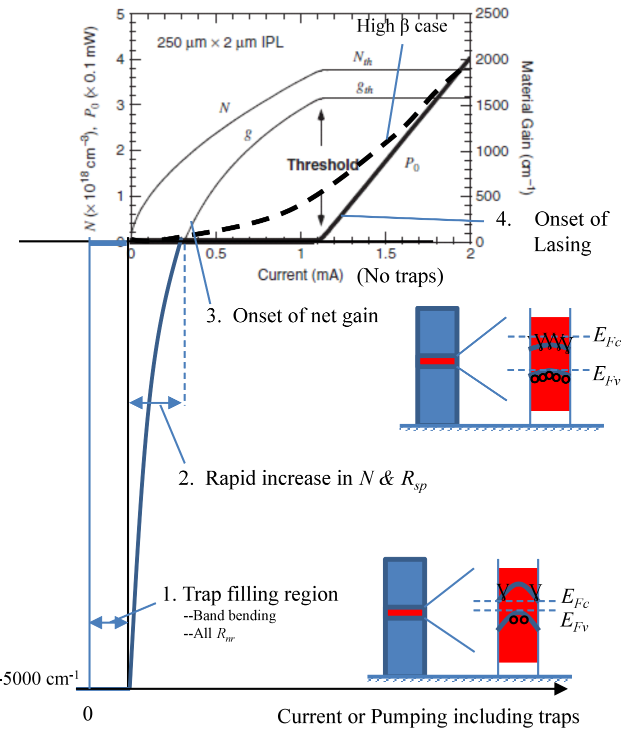

Figure 3. Plots of carrier density and gain vs pumping. Regions of trap filling (1), reduced absorption (2), gain (3) and lasing (4) indicated. Dashed *P-I* curve suggests the characteristic for a high β (~0.1) laser. Insets show schematics of nanolasers together with possible band structures for regions (1) and (3).

One method of determining β and also identifying the threshold of nanolasers has been to plot the *P—I* characteristic on a log-log scale, such as shown in Fig. 2. The ratio of the slope, *dP/dI*, above threshold to that below threshold from Eqns. (1) and (2) can be seen to equal $1/\eta_r\beta$. In Fig. 2, η_r is assumed to be unity. Unfortunately, in practical situations, η_r tends to become small in the same situations as when β is made large—i.e., in nanocavity devices, where surfaces and other defects often are nearby. As shown, β for ideal 2 µm^2 VCSELs is about 0.01, and it doesn't get larger than 0.1 until the cross section is considerably less than 1 µm^2.

Another issue in measuring such curves experimentally is that it is difficult to only capture a single mode below threshold, and this makes the slope ratio appear smaller, and β appear larger.

Figure 3 gives calculated gain and carrier density curves for the in-plane laser case. Also illustrated are some pitfalls that may occur if such material is used in nanocavities or some other structure where traps may exist. Although lasing doesn't actually occur until the region labeled #4, where the modal gain nearly equals the modal loss, the transition from region #1 to #2 can sometimes have a very distinct threshold, where the output light increases very sharply, and thereafter, its linewidth decreases substantially.

IV. SUMMARY

The classical characteristics for identifying lasing behavior are 1) a significant kink in the output light characteristic; 2) a narrowing of the output light spectrum; 3) perhaps some narrowing in the directivity of the emission; and 4) possibly some reduction in spontaneous emission in other directions. The first two are most widely used, and generally are used correctly. However, it is important to have a good idea of what the modal losses are in the laser, and if it is likely that the modal gain could possibly overcome these. Otherwise, one may not be observing lasing but perhaps a filling of traps or some other states, followed by spontaneous emission, maybe some filtering by the cavity, then possibly a reduction in loss and spectral narrowing with further pumping, etc., as discussed above.

It is also good to have some idea of what the laser linewidth should be for the power that is being generated. Although it is often difficult to measure the power accurately, it is important to get some estimate, so that it is possible to predict an order of magnitude linewidth that should be observed. The linewidth should be in the 10-40 MHz per mW, or 10-40 GHz per µW range. A nanometer (415 GHz @ 850nm) is still a pretty wide linewidth for a laser. Of course, this can be confused by chirping if the pumping is with short pulses.

In retrospect, one of my conclusions from the Rump Session was that it is very difficult to do better than well-engineered VCSELs for small, low-threshold, high-efficiency discrete devices. The main motivator to work on other structures appears to be to provide more efficient, compatible sources for planar photonic ICs.

REFERENCES

[1] L. A. Coldren, S. W. Corzine, M. L. Mašanović, Chapter 5, *Diode Lasers and Photonic Integrated Circuits—2nd Ed*., Wiley, New York, 2012.

Larry A. Coldren is the Fred Kavli Professor of Optoelectronics and Sensors at the University of California, Santa Barbara, CA. After receiving his Ph.D. Electrical Engineering from Stanford University and spending 13 years in research at Bell Laboratories, he joined UC-Santa Barbara in 1984 where he now holds appointments in Materials and Electrical & Computer Engineering. In 1990 he co-founded Optical Concepts, later acquired as Gore Photonics, to develop novel VCSEL technology; and in 1998 he co-founded Agility Communications, later acquired by JDSU, to develop widely-tunable integrated transmitters.

At Bell Labs Coldren worked on surface-acoustic-wave filters and later on tunable coupled-cavity lasers using novel reactive-ion etching (RIE) technology that he developed for the then new InP-based materials. At UCSB he continued work on multiple-section tunable lasers, in 1988 inventing the widely-tunable multi-element mirror concept, which is now used in numerous commercial products. Near this same time, he also made seminal contributions to efficient vertical-cavity surface-emitting laser (VCSEL) designs that continue to be implemented in practical devices. More recently, Prof. Coldren's group has developed high-performance InP-based photonic integrated circuits (PICs) as well as high-speed VCSELs, and they continue to advance the underlying materials growth and fabrication technologies.

Professor Coldren has authored or co-authored over a thousand journal and conference papers, a number of book chapters, a textbook, and has been issued 65 patents. He is a Fellow of the Institute of Electrical and Electronics Engineers, the Optical Society of America, and the Institute of Electronics Engineers (UK), a recipient of the 2004 John Tyndall and 2009 Aron Kressel Awards, and a member of the National Academy of Engineering.